

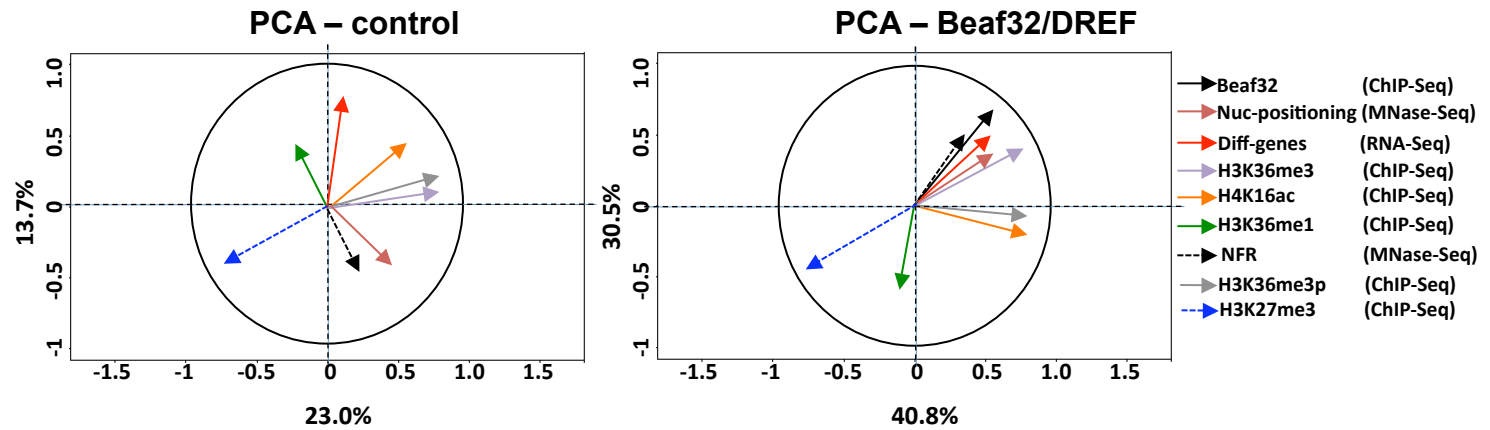
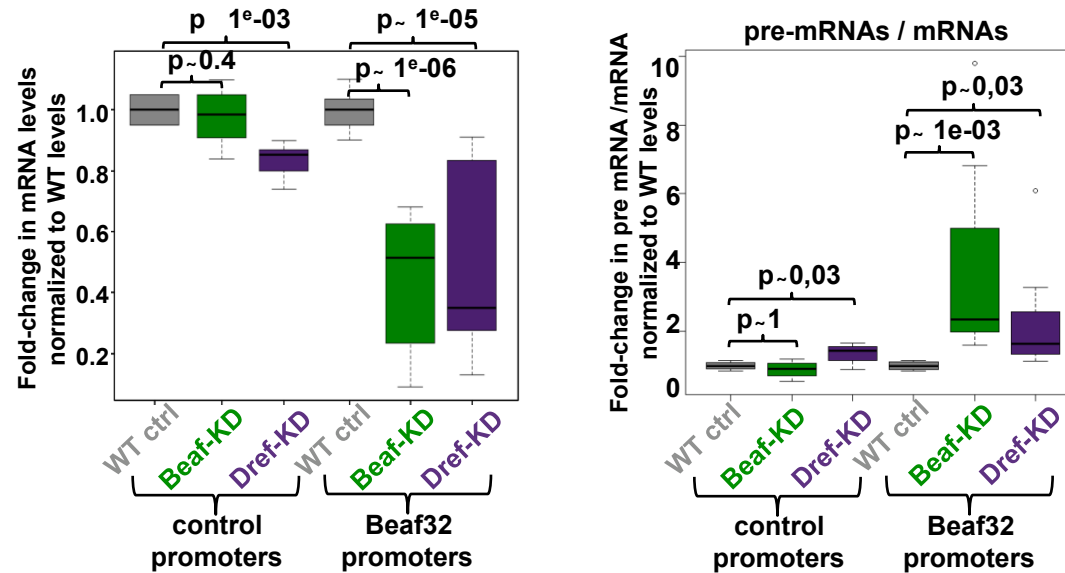
A**B**

Figure S9. Principal component analyses, RNA splicing defects upon depletion of Beaf32 or DREF.

A. Graph showing the genome-wide correlations as obtained by principal component analyses (PCA; see Methods)) among histone modifications and nucleosome positioning for genes that harbor or not a Beaf32/DREF binding site in their promoter (right and left panel, respectively). The y- and x- axis represent the two main dimensions. Note that to generate dendograms (see Figure 7A) by Clustering Ascendant Hierarchical (CAH) all additional PCA dimensions of significance are taken into consideration (Josse et al., 2011). All ChIP-Seq (Beaf32, H3K36me2/me3, H4K16ac, H3K27me3) and MNase-Seq (nucleosome-positioning, NFR) data were obtained from exponentially growing *Drosophila* cells. Note that the higher correlation between Beaf32/DREF binding and H3K36 methylation levels in gene bodies ('H3K36me3') as compared to promoter regions ('H3K36me3p') in agreement with the specific impact of Beaf32-KD in the former regions. Note also that H3K36me2/3 are anti-correlated with H3K27me3 marks, in agreement with data obtained in *C.elegans* or vertebrates (Gaydos et al., 2012; Cai et al., 2013). See also Figure 7A.

B. RNA splicing defects upon depletion of Beaf32 or DREF. Graph showing the results from RTqPCR measurements in triplicate showing the fold change (y-axis) in mRNA levels (left panel) or levels of immature RNAs normalized to mRNA (right panel). Immature RNAs were quantified using oligos that span exon-intron junctions in DREF-KD (purple boxes), Beaf32-KD (green boxes) as compared to control cells (grey boxes) for 16 genes (see Methods for a list) that harbor a Beaf32 binding site or not (see Methods for a list).